

1

2 **A silencer repressing redundant enhancer activities revealed by deleting**

3 **endogenous *cis*-regulatory element of *ebony* in *Drosophila melanogaster***

4

5 Noriyoshi Akiyama¹, Shoma Sato^{1, #}, Kentaro M. Tanaka¹, Takaomi Sakai¹, Aya Takahashi^{1,2*}

6

7 ¹ Department of Biological Sciences, Tokyo Metropolitan University, 1-1 Minamiosawa,
8 Hachioji 192-0397, Japan

9 ² Research Center for Genomics and Bioinformatics, Tokyo Metropolitan University, 1-1
10 Minamiosawa, Hachioji 192-0397, Japan

11

12

13

14

15 [#] Current Address:

16 Thermal Biology Group, Exploratory Research Center on Life and Living Systems, 5-1
17 Higashiyama, Myodaiji, Okazaki, Aichi, 444-8787, Japan

18

19 Division of Cell Signaling, National Institute for Physiological Sciences, 5-1 Higashiyama,
20 Myodaiji, Okazaki, Aichi, 444-8787, Japan

21

22

23

24 *Corresponding author

25 E-mail: ayat@tmu.ac.jp (AT)

26

27 **Abstract**

28

29 The spatiotemporal regulation of gene expression is essential to ensure robust phenotypic
30 outcomes. Pigmentation patterns in *Drosophila* are formed by the deposition of different pigments
31 synthesized in the developing epidermis and the role of *cis*-regulatory elements (CREs) of melanin
32 biosynthesis pathway-related genes is well-characterized. These CREs typically exhibit modular
33 arrangement in the regulatory region of the gene with each enhancer regulating a specific
34 spatiotemporal expression of the gene. However, recent studies have suggested that multiple
35 enhancers of a number of developmental genes as well as those of *yellow* (involved in dark pigment
36 synthesis) exhibit redundant activities. Here we report the redundant enhancer activities in the
37 *cis*-regulatory region of another gene in the melanin biosynthesis pathway, *ebony*, in the developing
38 epidermis of *Drosophila melanogaster*. The evidence was obtained by introducing an approximately
39 1 kbp deletion at the endogenous primary epidermis enhancer (priEE) by genome editing. The effect
40 of the priEE deletion on pigmentation and on the endogenous expression pattern of a
41 *mCherry*-tagged *ebony* allele was examined in the thoracic and abdominal segments. The expression
42 level of *ebony* in the priEE-deleted strains was similar to that of the control strain, indicating the
43 presence of redundant enhancer activities that drive the broad expression of *ebony* in the developing
44 epidermis. Additionally, the priEE fragment contained a silencer that suppresses *ebony* expression in
45 the dorsal midline of the abdominal tergites, which is necessary for the development of the subgenus
46 *Sophophora*-specific dark pigmentation patterns along the midline. The endogenous expression
47 pattern of *ebony* in the priEE-deleted strains and the reporter assay examining the autonomous
48 activity of the priEE fragment indicated that the silencer is involved in repressing the activities of
49 both proximal and distant enhancers. These results suggest that multiple silencers are dispensable in
50 the regulatory system of a relatively stable taxonomic character. The prevalence of other redundant
51 enhancers and silencers in the genome can be investigated using a similar approach.

52

53

54 **Author summary**

55

56 Genes are expressed at the right timing and place to give rise to diverse phenotypes. The
57 spatiotemporal regulation is usually achieved through the coordinated activities of
58 transcription-activating and transcription-repressing proteins that bind to the DNA sequences called
59 enhancers and silencers, respectively, located near the target gene. Most studies identified the
60 locations of enhancers by examining the ability of the sequence fragments to regulate the expression
61 of fused reporters. Various short enhancers have been identified using this approach. This study
62 employed an alternative approach in which the previously identified enhancer that regulates
63 expression of *ebony* (a gene involved in body color formation) was deleted in a fruitfly, *Drosophila*
64 *melanogaster*, using the genome-editing technique. The knockout of this enhancer did not affect the
65 transcription level of the gene to a large extent. This indicated the presence of
66 transcription-activating elements with redundant functions outside the deleted enhancer. Additionally,
67 the transcription of *ebony* at the midline of the abdomen, which is repressed in the normal flies, were
68 derepressed in the enhancer-deleted flies, which indicated that the deleted enhancer fragment
69 contained a silencer that negatively regulates multiple enhancer activities in a spatially restricted
70 manner.

71

72

73 **Introduction**

74 The spatiotemporal regulation of gene expression during the development of organisms
75 results in diverse phenotypes. The *cis*-regulatory elements (CREs) are nucleotides that differentially
76 modulate the transcription levels of specific genes typically in an allele-specific manner. The most
77 common CREs, enhancers and silencers, are located within a certain distance from the transcription
78 start sites of the target gene and contain binding sites for the transcription activators or repressors
79 [1,2]. Conventionally, the CREs comprising enhancers and silencers, which are unique to each
80 expression unit, are considered as subsets of modular structures in the upstream region of a gene [3–

81 7]. While this view reflects a fundamental principle since distinct CREs typically consist of clustered
82 binding motifs, there are recent evidences supporting a more complex picture. Various enhancers are
83 reported to exhibit functional redundancy or to cooperatively define the expression site boundaries
84 [8–14]. Also, a number of enhancers with pleiotropic functions have been reported (reviewed in
85 [15]).

86 The CREs in genes involved in body pigmentation pattern have been well-characterized
87 and multiple modular enhancers that activate transcription in different body regions have been
88 documented in detail (reviewed in [16,17]). For example, the distinct CREs of *yellow* that activate
89 transcription in bristles, wing and body, and abdomen have been identified [18–22]. However, a
90 recent study revealed that many sequence fragments in the regulatory region of *yellow* exhibit
91 redundant and cryptic enhancer activities, suggesting that *cis*-regulatory modules are not as distinct
92 as described previously and more amenable to evolutionary changes [23].

93 A complex architecture of *cis*-regulatory region has also been implicated from the
94 within-species comparisons of *cis*-regulatory sequences of *ebony*, another gene involved in body
95 pigmentation. Polymorphisms in *ebony*, which encodes an enzyme of the melanin biosynthesis
96 pathway, is the major causative factor determining the body pigmentation intensity in *D.*
97 *melanogaster* [24–27]. The sequence polymorphisms of the primary epidermis enhancer (priEE),
98 which was identified to be located in the upstream intergenic region of *ebony*, were analyzed in
99 detail. Some single-nucleotide polymorphisms (SNPs) first identified in the African populations
100 affected the enhancer function but were not associated with body pigmentation intensity in the
101 Japanese, European, North American, and Australian populations [27–32]. Also, a priEE haplotype
102 associated with light body color was identified in the Iriomote and Australian populations but not in
103 the African populations [32]. Furthermore, there were no SNPs or indels in the priEE that showed
104 complete association with the allele-specific expression levels in the developing epidermis in 20
105 strains sampled from the *Drosophila melanogaster* Genetic Reference Panel originated from a
106 natural population in North Carolina [28,33]. Moreover, some strains with identical priEE sequences
107 exhibited different allele-specific expression levels. These analyses suggest the possibility of the

108 presence of sequences outside the priEE region that regulate the expression level of *ebony*.

109 The priEE segment was the only segment within the approximately 10 kbp regulatory
110 region (including an upstream intergenic region and intron 1) that drove the expression of the
111 reporter gene in the epidermis [26]. However, the previous findings above have indicated that the
112 sequence variation within the priEE was not sufficient to explain the wide range of expression level
113 variation of this gene. Therefore, we hypothesized that similar to *yellow*, *ebony* has redundant
114 enhancers in addition to the priEE, possibly located outside the known approximately 10 kbp
115 regulatory region, and may be taking part redundantly in activating transcription of this gene in the
116 developing epidermis.

117 The expression pattern of *ebony* is repressed in certain areas of the abdomen of *D.*
118 *melanogaster*, which results in the generation of a distinct pigmentation pattern [26,34]. As the
119 transcription of *ebony* is simultaneously activated by multiple enhancers, silencing mechanisms must
120 be present to suppress the simultaneous activation. In *D. melanogaster*, dark stripes are visible in the
121 posterior regions of the A2–7 abdominal tergites in females and the A2–4 tergites in males. Also, the
122 abdominal pigmentation pattern exhibits sexual dimorphism with totally dark A5–7 tergites observed
123 only in males. Furthermore, another characteristic dark line is present along the dorsal midline of the
124 abdominal tergites in both males and females of this species. The dark line is a characteristic of the
125 subgenus *Sophophora* [35] and the expression of *ebony* is repressed in this region [26,34]. The
126 locations of silencers responsible for stripe repression and male-specific repression in the posterior
127 tergites have been suggested [26]. However, a silencer for repression at the dorsal midline has not
128 been identified previously.

129 The transgenic reporter assay is a powerful approach to dissect regulatory sequences and
130 identify CREs, such as enhancers and silencers. However, some limitations exist because this assay
131 does not test the sequence fragments in their native genomic environment [36]. Especially, the
132 lengths and borders of the sequence fragments can markedly affect the results [23]. In this study,
133 rather than conducting reporter gene assays, we examined the genomic region by modifying the
134 endogenous upstream sequence using the clustered regularly interspaced short palindromic repeats

135 (CRISPR)-CRISPR associated protein 9 (Cas9) system. The precise knockout of the known priEE in
136 a clean genetic background enabled the examination of its contribution to the body color phenotype.
137 We combined it with an assay using a reporter gene tagged to the endogenous *ebony* to capture the
138 changes in the expression pattern. As a result, we uncovered the presence of redundant enhancer
139 activities that drive the broad expression of *ebony* in the developing epidermis. We also show that
140 the priEE fragment contains silencers for repressing the expression of *ebony* in the dorsal midline of
141 the abdominal tergites, which is necessary for developing the *Sophophora*-specific pigmentation
142 pattern. This silencer represses the activities of the proximal and distant enhancers. We discuss the
143 consequences of such regulatory system on the evolution of CREs and the potential application of a
144 similar approach to other genomic regions.

145

146

147 **Results**

148 The priEE fragment was precisely knocked out using the CRISPR-Cas9 system to examine
149 whether transcriptional activation of *ebony* occurs in the absence of the priEE. First, to control the
150 genomic background, an isogenic Cas-0002 line (Cas-0002-iso) carrying the *nos*-Cas9 transgene was
151 constructed (Figs 1A and S1). Next, *mCherry* was knocked-in to the 3' end of *ebony* in the
152 Cas-0002-iso line using the CRISPR-Cas9 system (Fig 1B). The resultant transgenic line
153 (Cas-0002-iso_*e*::*mCherry*) was designed to produce a Ebony-mCherry fusion protein. Cas-0002-iso
154 and Cas-0002-iso_*e*::*mCherry* lines were crossed with guide RNA (gRNA) expression lines to drive
155 a targeted deletion at the approximately 970-bp priEE fragment [28,29] (Fig S2). Additional crosses
156 were performed to remove *y*² and replace the X chromosome with *w*^{III18} to avoid interference from
157 *yellow*, which is in the same pigment synthesis pathway (Fig S2). The following three priEE
158 deletions were generated; two from Cas-0002-iso line (*w*^{III18}; *e*^{A1088priEE} and *w*^{III18}; *e*^{A1089priEE}) and one
159 from Cas-0002-iso_*e*::*mCherry* line (*w*^{III18}; *e*^{A1077priEE}::*mCherry*) (Figs 1C–D). If the priEE contains
160 the only enhancer driving the expression of *ebony* in the epidermis, the priEE-deleted strains must
161 exhibit a dark body color equivalent to the *ebony* null mutant (*e*¹). Contrary to this prediction, the

162 body color of the priEE-deleted strains was similar to that of the control strain (Fig 2A).

163 The pigmentation intensity in the females of the two priEE-deleted strains ($w^{III8}; e^{A1088priEE}$
164 and $w^{III8}; e^{A1089priEE}$), the control strain ($w^{III8}; +$), and an *ebony* null mutant (e^l) was compared. The
165 percent darkness at the specific positions of the thoracic center and the fourth abdominal tergite (A4)
166 was measured (10 flies per strain) (Fig 2B–C). The pigmentation scores were significantly different
167 between the strains (thorax, $F_{3, 36} = 733.59$, $P < 10^{-15}$, one-way analysis of variance (ANOVA);
168 abdomen, $F_{3, 36} = 94.919$, $P < 10^{-15}$, one-way ANOVA). The thoraces of the two priEE-deleted
169 strains showed significantly but only slightly darker pigmentation than those of the control strain
170 (Fig 2B). The abdominal pigmentation in the $w^{III8}; e^{A1088priEE}$ strain was slightly lighter than that in
171 the control strain, but that in the $w^{III8}; e^{A1089priEE}$ strain was not significantly different from the
172 control strain (Fig 2C). These subtle changes in pigmentation intensity suggest that the priEE
173 deletion perturbs *ebony* transcription to some extent. However, the pigmentation in the thorax and
174 abdomen of the two priEE-deleted strains was markedly lighter than that in the thorax and abdomen
175 of e^l (Figs 2B–C). This indicated that deletion had limited effects on the overall transcription level
176 regulation. Hence, the priEE was shown to be dispensable for driving the transcription of *ebony* in
177 the developing epidermis.

178 Also, unexpectedly, the deletion of the priEE affected the pigmentation pattern. In
179 particular, the deletion of the priEE resulted in the loss of a dark pigmentation line along the dorsal
180 midline of the abdominal tergites (Fig 2A). This indicated that *ebony* expression is suppressed in the
181 midline area and that the priEE fragment is necessary for this suppression.

182 To directly investigate the expression sites of this gene in the abdomen, the abdominal
183 epidermis of the *mCherry* knocked-in strains, $w^{III8}; e::mCherry$ and $w^{III8}; e^{A1077priEE}::mCherry$ (Fig
184 1C), were subjected to fluorescence confocal microscopy (Figs 3A–B). The abdominal pigmentation
185 of $w^{III8}; e^{A1077priEE}::mCherry$ was consistent with the priEE-deleted strains without *mCherry* ($w^{III8};$
186 $e^{A1088priEE}$ and $w^{III8}; e^{A1089priEE}$) (data not shown), which suggested that the catalytic function of
187 *Ebony* in the pigmentation synthesis pathway is not disrupted upon fusion with *mCherry*.
188 Endogenous *ebony* exhibited a broad epidermal expression pattern (as expected from the light

189 pigmentation), and a suppressed expression at the posterior stripe region of each tergite (A1–6 of a
190 female and A1–4 of a male) and tergite-wide suppression at A5 and A6 in males (Figs 3A, D, and E).
191 These expression patterns were consistent with those reported in previous studies [17,34]. As
192 predicted from the pigmentation scores in Fig 2A, *ebony* expression in w^{1118} ; $e^{A1077priEE}::mCherry$
193 was similar to that in the control strain except that the expression at the dorsal midline was not
194 suppressed (Figs 3B, D, and E). These results indicate that the enhancer activity resides outside the
195 primary enhancer and that redundant enhancer element(s) is present in the surrounding genomic
196 region. The expression of *ebony* has been reported in other body regions [26,37–39] but the priEE
197 has not been indicated to drive expression in tissues other than the developing epidermis [26]. As
198 expected, the expression patterns of *ebony* did not markedly change in other tissues upon deletion of
199 the priEE (Fig S3).

200 The results indicated that the deleted priEE fragment contained a silencer element for the
201 dorsal midline as well as an epidermal enhancer element. In order to confirm that the deleted priEE
202 contains both elements, a GFP reporter assay was performed. The priEE fragment was fused to an
203 enhanced GFP (*EGFP*) gene (*priEE-EGFP*) with a minimal Hsp70 promoter and transformed into
204 two attP strains (VK00033 and VK00037). The confocal images of GFP from *priEE-EGFP*
205 transformed to a third chromosome landing site in VK00033 (Figs 3C and E) and a second
206 chromosome landing site in VK00037 (Fig S4) indicated that the priEE autonomously drives the
207 epidermal expression except at the flanking regions of the dorsal midline. Rebeiz *et al.* [26] reported
208 that the 0.7 kbp core element (included in the approximately 970-bp priEE) drove a similar
209 expression pattern. The pattern clearly showed that a dorsal midline silencer is present in the priEE
210 fragment and that it can silence the activity of the proximal enhancer element within the priEE
211 fragment, which drives the broad expression of *ebony* in the developing abdominal epidermis.

212

213

214 **Discussion**

215 **Redundant enhancer activity resides in the regulatory region of *ebony***

216 The removal of the endogenous priEE of *ebony* using the CRISPR-Cas9 system did not
217 cause a drastic darkening as observed in the null mutant (*e*¹), although a slight perturbation of the
218 pigmentation intensities in the thoracic and abdominal segments was observed (Fig 2). A strong
219 negative correlation between the darkness of body pigmentation and the expression level of *ebony* in
220 the developing epidermis has been repeatedly detected in strains sampled from the natural
221 populations of *D. melanogaster* [24–29]. Thus, the dark pigmentation intensity of the cuticle is
222 suggested to be a sensitive indicator of local changes in the expression level of *ebony*. Therefore, the
223 lack of a large increase in dark pigmentation in strains with the priEE deletion indicated that
224 transcription of the gene was not largely disrupted. Further, these findings indicated that the
225 transcriptional activation of *ebony* in the developing epidermis can also be driven by the endogenous
226 sequences outside the priEE, suggesting the presence of redundant enhancer elements in the
227 surrounding genomic region. The complex arrangement of multiple CREs may be a reason for the
228 scarcity of polymorphisms association with pigmentation intensity or gene expression level within or
229 near the enhancer element across worldwide populations [32].

230 The locations of the redundant elements have not been determined. The results of a
231 previous reporter assay revealed that no fragments other than those including the priEE segment
232 were detected within the approximately 10 kbp regulatory region that contains the 5' intergenic
233 region and the first intron [26]. Therefore, redundant enhancer elements are likely to be located
234 elsewhere. However, unlike the recent reporter assay conducted with the *yellow* regulatory region
235 [23], many regions were tested using relatively large fragments (> 2 kbp), which may contain cryptic
236 enhancers that are repressed by surrounding sequences in their native genomic context. Therefore,
237 the possibility of the presence of redundant enhancer elements within the approximately 10 kbp
238 regulatory region cannot be ruled out. Some secondary enhancers are reported to be shadow
239 enhancers that are more than 20 kbp away from the transcription start site [8]. Thus, there is a need
240 for extensive search to elucidate the detailed spatial arrangement of CREs. Nevertheless, the
241 advantage of deleting an endogenous enhancer, a strategy employed in this study, is the rapid
242 capturing of redundant enhancer activity in the native genomic context. Such knockout assays using

243 endogenous genome editing may reveal more cases of redundant enhancer activities in the
244 *Drosophila* genome as in the study conducting similar experiments on mouse developmental genes
245 [40]. Moreover, this approach can compensate for some potential bias in reporter gene assays caused
246 by the choice of promoter and the genomic location of the transgenes [36].

247

248 **Possible functions of redundant enhancers are to be investigated**

249 Redundant enhancer elements, which are often referred to as primary and shadow
250 enhancers [8], have been suggested to confer robustness against environmental or genetic
251 perturbations [10,12,39] or define sharp boundaries for gene expression [11,13]. The transcriptional
252 activation of *ebony* by multiple enhancers appears to be largely overlapping but may not be
253 completely redundant, considering the subtle changes in the pigmentation intensity upon deletion of
254 the priEE (Fig 2B). However, wide range of variations in the transcription level of this gene have
255 been reported within and among *D. melanogaster* populations [24–29]. Thus, maintaining a robust
256 transcription level of this gene might not be essential. The functional significance of redundant
257 enhancers in this gene requires further investigation.

258

259 **A single silencer represses the activity of multiple redundant enhancers**

260 Spatially restricted suppression of focal gene transcription can be achieved by introducing
261 a specific silencer that recruits repressive transcription factors (or repressors) expressed in the target
262 cells. In contrast to enhancers, there is far limited information on the exact locations and features of
263 silencers. This study demonstrated that the priEE fragment contained a silencer of *ebony* expression
264 in the abdominal dorsal midline based on two experimental evidences. First, the suppression of
265 *ebony* expression at the dorsal midline was not observed when the priEE fragment was deleted (Figs
266 2A and 3B). Second, experiments with priEE fragment fused to a reporter gene revealed a broad
267 epidermal expression driven by autonomous enhancer activity and the suppression of gene
268 expression at the dorsal midline (Fig 3C). These results also have implications about the functional
269 category of the silencer in accordance to its effective range.

270 The repressors can be grouped into the following two categories: short-range repressors,
271 locally inhibit activators at distances of less than 100–150 bp, long-range repressors, inhibit
272 activators at distances of at least 500 bp or longer [41–43]. Generally, long-range repressors can
273 function in a dominant fashion to block multiple enhancers [41]. The *ebony* expression in the
274 priEE-deleted strain implies that in the wildtype strain, when the silencer is intact, multiple
275 enhancers of this gene are simultaneously inhibited. The results of the *priEE-EGFP* reporter assay
276 demonstrated that the repressor bound to the silencer within the fragment interferes with the
277 proximal enhancer, and may exhibit short-range repression. Taken together, a single silencer is
278 sufficient to inhibit all the redundant activities from the proximal and distant enhancers, possibly by
279 interfering with the basal transcription machinery at the promoter site. Also, the repressor bound to
280 this silencer might have a potential to directly interact with the proximal enhancer element at
281 short-range. Various models have been described to explain the long-range and short-range functions
282 of repressors [41–45]. A chromatin conformation analysis may be effective to identify the direct
283 physical interaction between the silencer and the promoter.

284 A schematic representation of the *cis*-regulatory transcriptional control of this gene is
285 shown in Fig 3F. As incorporated in the model, the repression of *ebony* in the dark stripes at the
286 posterior regions of the abdominal tergites and the totally dark A5–6 tergites in males is not affected
287 (Figs 3A–D). This is consistent with the results of a previous study, which showed that the locations
288 of these silencers are not within the deleted fragment [26]. The authors revealed that the male
289 silencer was located approximately 1.5 kbp upstream of the transcription start site, and the stripe
290 silencer was located within the first intron. Whether these CREs recruit long-range and/or
291 short-range repressors or not would be an intriguing question for obtaining a comprehensive picture
292 of the regulatory system of this gene. A similar approach to remove the putative silencer region can
293 be effective for the purpose.

294 At the molecular level, *omb*, *dpp*, and *wg*, are reported to be involved in the formation of
295 sexually monomorphic pigmentation patterns in the abdomen of *D. melanogaster*, and *dpp*, which is
296 expressed at the dorsal midline is essential for the formation of dark pigmentation along the midline

297 [46–48]. Additionally, *dpp* is known to activate the BMP signaling pathway, which regulates the
298 transcription of numerous genes through a downstream transcription factor Mad (reviewed in [49]).
299 Kopp *et al.* [46] showed that *Mad*¹² clones at or near the dorsal midline promoted the loss of dark
300 pigmentation, which suggested that Dpp signaling contributes to pigmentation. Furthermore, an
301 RNAi screening revealed that 48 transcription factors, including Mad, are involved in abdominal
302 pigmentation [50]. Therefore, it is likely that the suppression of *ebony* by the silencer is regulated
303 through the Dpp signaling pathway.

304

305 **Derepression of *ebony* is sufficient to diminish a taxonomic character**

306 In the genus *Drosophila*, the pigmentation pattern of the abdominal midline is one of the
307 traits used to classify the subgenus *Sophophora*, which includes *D. melanogaster*, and the subgenus
308 *Drosophila*. With some exceptions, the pigmentation stripes on the abdominal tergites of the
309 subgenus *Sophophora* are mostly connected or expanded anteriorly at the dorsal midline forming a
310 distinct dark area along the midline as in *D. melanogaster* (Figs 2A and 3D). In contrast, the stripes
311 are narrowed or broken at the midline in most species of the subgenus *Drosophila* [35]. We have
312 shown that the suppression of *ebony* by the abdominal midline silencer is at least necessary for the
313 *Sophophora*-type midline to appear in *D. melanogaster*. The expression patterns of *pale*, *Ddc*, *ebony*,
314 *tan*, and *yellow* in the developing abdominal epidermis of species belonging to subgenus
315 *Sophophora* were previously examined using *in situ* hybridization [34]. Among the investigated
316 genes, the suppression of *ebony* appears to be most pronounced in species with a typical dark dorsal
317 midline.

318 A pair of sister species within the subgenus *Drosophila*, *D. americana* and *D.*
319 *novamexicana*, represents another case of distinct pigmentation patterns in the abdominal midline. *D.*
320 *americana* has a dark body color with uniformly dark abdominal tergites, whereas *D. novamexicana*
321 exhibits a light pigmentation along the abdominal midline [51], which is a typical pattern of the
322 subgenus. A recent study used reciprocal hemizygosity testing to demonstrate that the difference in
323 abdominal midline pigmentation intensity between the two species was due to *ebony* [52]. The

324 authors showed that *ebony* is required for the development of light pigmentation along the dorsal
325 midline in wild-type *D. novamexicana*. It has not been demonstrated whether the interspecific
326 differences of *ebony* resides in the *cis*-regulatory region or not. However, the study also suggests that
327 *ebony* suppression might be a key factor for determining this taxonomically important trait.

328 In this study, a single silencer was sufficient to suppress the activities of multiple
329 enhancers in the *cis*-regulatory region of *ebony*. This long-range repression eliminates the need for
330 an acquisition of repressor-binding sites for individual enhancer elements. A study of *yellow*, which
331 is also expressed in the developing epidermis, from three different species revealed a contrasting
332 picture of frequent evolutionary acquisition and loss of short-range repressor binding sequences [23].
333 Also, reporter assays examining the effect of the male-specific silencer of *ebony* in *D. auraria* and *D.*
334 *serrata* observed a frequent loss of this silencer in these species [53]. The differences in silencer
335 properties may be attributed to the evolutionary stability of the focal expression sites. The presence
336 of a universal silencer may be prevalent in genes responsible for relatively stable taxonomic
337 characters that delimit certain clades of species. Such silencers enable the redundant enhancer
338 elements to fine-tune their regulation while maintaining robust transcription suppression in a
339 spatially restricted manner.

340 These findings, together with the recently accumulating evidences of redundant CREs,
341 suggest that the architectures of *cis*-regulatory regions are diverse and the possible evolutionary
342 regimes may be more complex and variable than the conventional view of modularly restricted
343 evolution of CREs.

344

345

346 Materials and Methods

347 Fly strains

348 y^2 , cho^2 , v^I , P{*nos*-Cas9, y^+ , v^+ }1A/FM7c, Kr-GAL4, UAS-GFP (Cas-0002), y^I , v^I ,
349 P{*nos*-phiC31 λ int.NLS}X; attP40 (II) (TBX-0002), y^2 , cho^2 , v^I ; *Sco/CyO* (TBX-0007), and y^2 , cho^2 ,
350 v^I ; *Pr*, *Dr/TM6C*, *Sb*, *Tb* (TBX-0010) lines were obtained from the NIG-FLY Stock Center. w^{118} ;

351 $wg^{Sp-1}/CyO; Pr^I Dr^I/TM3 Sb^I Ser^I$ (DGRC#109551) and e^1 (DGRC#106436) were obtained from
352 the Kyoto Stock Center. The isogenized Cas-0002 strain (Cas-0002-iso) was established via the
353 triple balancer by crossing DGRC#109551 with Cas-0002 (Fig S1). The TBX-double-balancer (y^2 ,
354 $cho^2, v^I; Sco/CyO; Pr, Dr/TM6C, Sb, Tb$) was generated from TBX-0007 and TBX-0010. The two
355 attP strains $y^I w^{III8}$; PBac{ y^+ -attP-3B}VK00033 (DGRC#130419) and $y^I w^{III8}$;
356 PBac{ y^+ -attP-3B}VK00037 (DGRC#130421) were used to generate transgenes at WellGenetics. All
357 fly stocks were reared at 25°C on a standard corn-meal fly medium.

358

359 **Repair construct for *mCherry* knock-in**

360 The repair construct (Fig 1B) was designed following the method described by Hinaux *et*
361 *al.* [54]. The construct *pJet-yellow_F4mut-mCherry* was gifted from Dr. Nicolas Gompel. A part of
362 the *ebony* locus (2,610 bp (from approximately 1 kbp upstream of exon 7, to approximately 1 kbp
363 downstream of 3'UTR)) was amplified from Cas-0002-iso (Fig 1A) using primers with the XhoI,
364 (5'-AGCctcgagTGGTGGATAAGGCCATTGTT-3') and XbaI (5'-
365 CAGtctagaTGCAACTGGTTGTGCGTAT-3') digestion sites. PCR was performed using KAPA
366 HiFi HotStart ReadyMix (Kapa Biosystems). The *pJet-yellow_F4mut-mCherry* vector was digested
367 with XhoI and XbaI and the fragments flanked by these digestion sites (including partial *yellow* and
368 *mCherry* gene sequences) were replaced by the PCR product, which was digested with the same
369 restriction enzymes. The complete sequence of the resulting vector, excluding the *ebony* termination
370 codon, was PCR-amplified using the following primers: 5'-GACGACCACCCGGTGGACGT-3' and
371 5'-TTTCCCCACCTCCTTCCAAT-3'.

372 Next, the *mCherry* sequence with a 5' linker [55] was amplified from the
373 *pJet-yellow_F4mut-mCherry* vector using primers with 15 bp homologous flanking sequences
374 (5'-AAGGAGGTGGCAAAGGATCCGCTGGCTCCGCTGCTG-3' and
375 5'-CACCGGGTGGTCGTCTTACTTGTACAGCTCGTCCATGCC-3'). These two amplicons were
376 fused using the In-Fusion HD Cloning Kit (TaKaRa) to generate the *pJet-ebony-mCherry* vector.

377 Finally, the two synonymous mutations were inserted at the target sequence of gRNA
378 (5'-GCGCGCTATTGTCCATTGGA-3') to reduce the risk of the repair construct being cut during the
379 knock-in reaction. To induce mutations, two overlapping amplicons, including the gRNA target
380 sequence, from the *pJet-ebony-mCherry* vector were generated using PCR with the following primer
381 pairs: 5'-AATCCCCGCGAGAACATC-3' and 5'-TCCAGTGTACAATAGCGCGC-3';
382 5'-GCGCTATTGTACACTGGAAG-3' and 5'-TTGTCTGGAAATCAAAGGCTTA-3'. These two
383 PCR products were connected using overlap extension PCR to generate a mutated fragment. This
384 mutated fragment was replaced by the original homologous sequence of the
385 *pJet-ebony_mut-mCherry* vector by fusing the mutated fragment and the PCR product amplified
386 from the *pJet-ebony-mCherry* vector using the In-Fusion HD Cloning Kit (TaKaRa) with the
387 following primers: 5'-GCCTTGATTTCCAGACAA-3' and 5'-GTTCTCGCGGGGATTCAAC-3'.
388 The constructed *pJet-ebony_mut-mCherry* vector was used as the repair construct for *mCherry*
389 knock-in.

390

391 **gRNA vector cloning**

392 All the guide sequences of gRNAs were cloned into the pCFD5 vector (Addgene ##73914)
393 according to the pCFD5 cloning protocol [56]. The guide sequences of gRNA1
394 (5'-GGAGCACGAGGTTCTGCGGG-3') and gRNA2 (5'-GCGCGCTATTGTCCATTGGA-3') were
395 designed within exon 7 of *ebony* and cloned into separate pCFD5 vectors. The guide sequences of
396 gRNA3 (5'-GTTAATAAGATCGGACAGAC-3') and gRNA4
397 (5'-GAAAGTACTATCAATATACA-3'), which were designed at both ends of the approximately
398 970-bp priEE fragment (Fig S5, [28,29]), were cloned into a single plasmid. An In-Fusion HD
399 Cloning Kit (TaKaRa) was used for cloning.

400

401 **Construct for reporter gene assay**

402 The sequence of the priEE of *ebony* was amplified from Cas-0002-iso (Fig 1B) using the
403 following primers with restriction enzyme digestion sites:

404 5'-CGGgaattcGGGCAAAGCAGGGTGAATA-3' (EcoRI site) and
405 5'-ACTgcggccgcTCACAGGGACTTATGGGAAA-3' (NotI site). These primers were designed to
406 amplify most of the priEE knocked out sequences including the whole *e_ECR0.9* [29] and
407 *e_core_cis* [28] elements (Fig S5). The amplified product and the pEGFP-attB vector with a minimal
408 Hsp70 promoter (*Drosophila* Genomics Resource Center) were digested with EcoRI and NotI. The
409 PCR product was cloned into the multi-cloning site of the vector.

410

411 **Embryonic microinjection**

412 For *mCherry* knock-in, an *ebony* knockout strain was generated by injecting the gRNA1
413 guide-sequence-cloned pCFD5 vector (200 ng/μl) into the embryos of Cas-0002-iso. The embryos of
414 *ebony* knockout strain were injected with a mixture of the gRNA2 guide-sequence-cloned pCFD5
415 vector (200 ng/μl) and the repair construct *pJet-ebony_mut-mCherry* (400 ng/μl). Of the 250 adult
416 flies that emerged from the injected embryos, four restored wild-type body color. The sequences of
417 exon 7 of *ebony* and knocked-in *mCherry* were confirmed using Sanger sequencing with a
418 BrilliantDye Terminator cycle sequencing kit (NimaGen) and an ABI PRISM 3130xl Genetic
419 Analyzer (Applied Biosystems). The established strain was named Cas-0002-iso_*e::mCherry* (Fig
420 1B).

421 The pCFD5 vector with guide sequences of gRNA3 and gRNA4 (200 ng/μl) was injected
422 into the embryos of TBX-0002. The gRNA expression strain (y^2 , *cho*², *v*¹; attP40{gRNA, *v*⁺}; *Pr*,
423 *Dr/TM6c, Sb, Tb*) was established by mating the successfully transformed individual with the
424 TBX-double-balancer. The guide sequences of gRNAs of the established strains were confirmed
425 using Sanger sequencing with a BrilliantDye Terminator cycle sequencing kit (NimaGen) and an
426 ABI PRISM 3130xl Genetic Analyzer (Applied Biosystems).

427 The pEGFP-attB vector with the priEE fragment was prepared at a high concentration
428 using Plasmid Midi Kit (Qiagen) and transported to WellGenetics (Taiwan) for injection into two
429 attP strains (y^1 *w*¹¹¹⁸; PBac{*y*⁺-attP-3B}VK00033 and y^1 *w*¹¹¹⁸; PBac{*y*⁺-attP-3B}VK00037).

430

431 **Deletion strains generated by CRISPR-Cas9**

432 The deletion strains were established by crossing gRNA expression strains with
433 Cas-0002-iso or Cas-0002-iso_ *e::mCherry* (the mating scheme shown in Fig S2). Deletions (Dels)
434 occur in the germline cells of G1. Twelve G1 males were crossed one by one with several TBX-0010
435 virgin females. Eight G2 males sampled from the progenies of each G1 male were subjected to PCR
436 screening. DNA samples extracted from the mid-legs of G2 males were amplified using the primers
437 e_-5029F (5'-CGTGTGCCTGATCGCTAGA-3') and e_-3391R
438 (5'-ACTCGTGCCTTACTTAATCTGAA-3'), which were designed to amplify the target region. The
439 G2 individuals were screened by subjecting the amplicons to electrophoresis using a 1% agarose gel.
440 G2 individuals with deletions were crossed again with TBX-0010. Then, G3 (*y*², *cho*², *v*¹; +;
441 *Del/TM6c, Sb, Tb*) individuals were crossed with each other to establish G4 homozygous strains (*y*²,
442 *cho*², *v*¹; +; *Del*). The deletions were confirmed using Sanger sequencing with a BrilliantDye
443 Terminator cycle sequencing kit (NimaGen) and an ABI PRISM 3130xl Genetic Analyzer (Applied
444 Biosystems). The males from the homozygous deletion strains (G4) were crossed twice with the
445 double balancer *w*^{III8}; *wg*^{Sp-1}/ *CyO*; *Pr*¹, *Dr*¹/ *TM3, Sb*¹, *Ser*¹ (DGRC#109551) to replace the *y*², *cho*²,
446 *v*¹ X chromosome. Finally, the G7 homozygous deletion strains (*w*^{III8}; +; *Del*) were established (Fig
447 S2). Control strains (*w*^{III8}; +; + and *w*^{III8}; +; *e::mCherry*) were established with the same crosses
448 using TBX-0002 instead of the gRNA expression strain (Fig S2).

449

450 **Quantification of pigmentation intensity**

451 At 5–7 days after eclosion, females were placed in 10% glycerol in ethanol at 4°C for 1 h.
452 Next, the flies were rotated in 10% glycerol in phosphate-buffered saline (PBS) at room temperature
453 for 1 h after removing the head, legs, and wings. The images of the dorsal body of flies soaked in
454 10% glycerol in PBS were captured using a digital camera (DP73, Olympus) connected to a
455 stereoscopic microscope (SZX16, Olympus). The same parameters (exposure time, zoom width and
456 illumination) and reference grayscale (brightness = 128; ColorChecker, X-rite) were applied for
457 capturing all images. White balance was corrected using the white scale (Brightness = 255;

458 ColorChecker, X-rite) with cellSens Standard 1.6 software (Olympus). Pigmentation intensity was
459 measured in manually selected areas of the thorax and abdomen (Figs 2 B and C) from RGB images
460 of flies using ImageJ 1.53a [57]. The mode grayscale brightness values from thorax and abdomen
461 were corrected using the reference grayscale of the background area at the bottom left corner of each
462 image. The percent of darkness was calculated as follows:

$$\left(1 - \frac{\text{brightness}}{\text{background brightness}} \times \frac{128}{255}\right) \times 100 (\%)$$

463 The raw measurement data are in Table S1. The data were analyzed using one-way
464 ANOVA, followed by Tukey HSD post-hoc test. Statistical analyses were performed using R version
465 4.0.3 [58].

466

467 **Confocal microscopy**

468 The adult flies were dissected 4 h after eclosion and the abdomen, wings, front legs, and
469 halteres were collected in PBS. The dorsal abdominal cuticle and epidermis were separated from the
470 rest of the abdomen. The fat body, internal organs, and genitalia were gently removed. The head of
471 adult females collected at 4–4.5 h after the light was turned on was dissected in PBS and the intact
472 brain was obtained. Each brain sample was fixed in 4% paraformaldehyde for 1 h and washed with
473 PBS for 1 h after fixation.

474 Each specimen was mounted with VECTASHIELD Mounting Medium with DAPI (Vector
475 Laboratories) and imaged under a C2 plus confocal microscope (Nikon). Max intensity images were
476 composited from the XY overlapping images (abdomen: 12 images, wing: 10 images) with 1 μm
477 wide Z-stacks using the NIS Elements AR 4.50.00 software. The following laser wavelengths were
478 applied for obtaining images: 488 nm activation wavelength and 509 nm imaging wavelength for
479 EGFP imaging; 561 nm activation wavelength and 620 nm imaging wavelength for mCherry. The
480 identical parameters of C2 plus settings (HV, offset, laser power, pinhole size, scan size, scan speed,
481 scan direction, and zoom) were applied for imaging the same fluorescence in the same tissue
482 (mCherry or EGFP). No further corrections were applied.

483

484 **Supporting Information**

485 **Table S1 Raw pigmentation scores (10 females per strain) of the strains used in this study**

486

487 **Fig S1 Scheme for extracting an isogenized chromosome**

488 To control for the genetic background of the genome-edited flies, each chromosome was originated
489 from a single chromosome. The isogenized strain was named Cas-0002-iso.

490

491 **Fig S2 Scheme for generating primary enhancer element (priEE) deletion strains without y^2**

492 CRISPR-Cas9-based genome editing was performed by crossing the Cas-0002-iso with the guide
493 RNA (gRNA) expression strain (G0). The progenies from the G1 cross were screened for the
494 presence of deletions. Homologous deletions were achieved by the crosses in G3 and G4. y^2 was
495 removed by the crosses in G4 to G7 because it interferes with *ebony* in the pigment biosynthesis
496 pathway. Deletion strains for mCherry fluorescence observation were established using the same
497 scheme, except Cas-0002-iso-*e::mCherry* was used instead of Cas-0002-iso (G0). Control strains
498 ($w^{1118}; +; +$ and $w^{1118}; +; e::mCherry$) were established with the same crosses using TBX-0002
499 instead of the gRNA expression strain and using + instead of the Del genotype for the G2 cross.

500

501 **Fig S3 *ebony* expression in tissues other than developing epidermis**

502 Confocal images of brain (A and B), front leg (C and D), wing (E, E', F and F'), and haltere (G and
503 H). Each tissue was dissected from the control, $w^{1118}; e::mCherry$ (A, C, E, E' and G), and the
504 priEE-deleted strain $w^{1118}; e^{A1077priEE}::mCherry$ (B, D, F, F' and H). (E') and (F') are magnified views
505 of the yellow square in (E) and (F), respectively. The scale bars indicate 100 μ m.

506

507 **Fig S4 Reporter assay using the enhanced GFP-tagged primary enhancer element**

508 **(priEE-EGFP) construct in the developing abdominal epidermis**

509 Confocal fluorescence images of the developing abdominal epidermis of *priEE-EGFP* transformed
510 to VK00037. Images of females and males are shown in the upper and lower panels, respectively.

511 Scale bars indicate 500 μ m.

512

513 **Fig S5 Alignment of sequences around the primary enhancer element (priEE) in the control**
514 **and priEE knockout strains**

515 The guide RNA (gRNA) target sequences are indicated above the sequence. Bases in bold indicate
516 the 947-bp sequence of *e_ECR0.9* from Takahashi and Takano-Shimizu [29] (969-bp sequence in the
517 control strain (Cas-0002-iso-derived *w¹¹¹⁸*; + strain)). Bases in blue indicate the 961-bp sequence of
518 *e_core_cis* sequence from Miyagi *et al.*[28] (975 bp in the control strain (Cas-0002-iso-derived
519 *w¹¹¹⁸*; + strain)). Shaded bases indicate the sequence fragment (1,047 bp) used for the reporter assay
520 in this study.

521

522 **Acknowledgment**

523 We would like to thank Nikolas Gompel for *pJet-yellow_F4mut-mCherry* vector, WellGenetics for
524 embryonic injection, and NIG-Fly and Kyoto Stock Center for fly stocks. We would like to thank
525 Koichiro Tamura and the Evolutionary Genetics Laboratory members at TMU for critical comments
526 and discussions. The work was partly supported by the Sasakawa Scientific Research Grant (No.
527 2019-4038) from The Japan Science Society and by JSPS KAKENHI (Grant No. JP19H03276)
528 awarded to N.A. and A.T., respectively.

529

530 **Author contributions**

531 Conceived and designed the experiments: NA KMT AT.
532 Performed the experiments: NA SS.
533 Analyzed the data: NA SS.
534 Contributed reagents/materials/analysis tools: KMT TS AT.
535 Wrote the paper: NA AT.

536

537 **References**

538 1. Spitz F, Furlong EEM. Transcription factors: From enhancer binding to developmental control.
539 Nat Rev Genet. 2012;13: 613–626. doi:10.1038/nrg3207

540 2. Long HK, Prescott SL, Wysocka J. Ever-changing landscapes: transcriptional enhancers in
541 development and evolution. Cell. 2016;167: 1170–1187. doi:10.1016/j.cell.2016.09.018

542 3. Arnone MI, Davidson EH. The hardwiring of development: organization and function of genomic
543 regulatory systems. Development. 1997;124: 1851–1864.

544 4. Stern DL. Perspective: Evolutionary developmental biology and the problem of variation.
545 Evolution. 2000;54: 1079–1091. doi:<https://doi.org/10.1111/j.0014-3820.2000.tb00544.x>

546 5. Wray GA, Hahn MW, Abouheif E, Balhoff JP, Pizer M, Rockman M V, et al. The evolution of
547 transcriptional regulation in eukaryotes. Mol Biol Evol. 2003;20: 1377–1419.
548 doi:10.1093/molbev/msg140

549 6. Prud'homme B, Gompel N, Carroll SB. Emerging principles of regulatory evolution. Proc Natl
550 Acad Sci. 2007;104: 8605–8612. doi:10.1073/pnas.0700488104

551 7. Carroll SB. Evo-devo and an expanding evolutionary synthesis: a genetic theory of morphological
552 evolution. Cell. 2008;134: 25–36. doi:10.1016/j.cell.2008.06.030

553 8. Hong JW, Hendrix DA, Levine MS. Shadow enhancers as a source of evolutionary novelty.
554 Science. 2008;321: 1314. doi:10.1126/science.1160631

555 9. Perry MW, Boettiger AN, Bothma JP, Levine M. Shadow enhancers foster robustness of
556 *Drosophila* gastrulation. Curr Biol. 2010;20: 1562–1567.
557 doi:<https://doi.org/10.1016/j.cub.2010.07.043>

558 10. Perry MW, Cande JD, Boettiger AN, Levine M. Evolution of insect dorsoventral patterning
559 mechanisms. Cold Spring Harb Symp Quant Biol. 2009;74: 275–279.
560 doi:10.1101/sqb.2009.74.021

561 11. Perry MW, Boettiger AN, Levine M. Multiple enhancers ensure precision of gap gene-expression
562 patterns in the *Drosophila* embryo. Proc Natl Acad Sci U S A. 2011;108: 13570–13575.

563 doi:10.1073/pnas.1109873108

564 12. Frankel N, Davis GK, Vargas D, Wang S, Payre F, Stern DL. Phenotypic robustness conferred by
565 apparently redundant transcriptional enhancers. *Nature*. 2010;466: 490–493.
566 doi:10.1038/nature09158

567 13. Bothma JP, Garcia HG, Ng S, Perry MW, Gregor T, Levine M. Enhancer additivity and
568 non-additivity are determined by enhancer strength in the *Drosophila* embryo. Krumlauf R, editor.
569 *Elife*. 2015;4: e07956. doi:10.7554/eLife.07956

570 14. El-Sherif E, Levine M. Shadow enhancers mediate dynamic shifts of gap gene expression in the
571 *Drosophila* embryo. *Curr Biol*. 2016;26: 1164–1169.
572 doi:<https://doi.org/10.1016/j.cub.2016.02.054>

573 15. Sabarís G, Laiker I, Preger-Ben Noon E, Frankel N. Actors with multiple roles: pleiotropic
574 enhancers and the paradigm of enhancer modularity. *Trends Genet*. 2019;35: 423–433.
575 doi:10.1016/j.tig.2019.03.006

576 16. Massey JH, Wittkopp PJ. The genetic basis of pigmentation differences within and between
577 *Drosophila* species. *Curr Top Dev Biol*. 2016;119: 27–61. doi:10.1016/bs.ctdb.2016.03.004

578 17. Rebeiz M, Williams TM. Using *Drosophila* pigmentation traits to study the mechanisms of
579 *cis*-regulatory evolution. *Curr Opin Insect Sci*. 2017;19: 1–7.
580 doi:<https://doi.org/10.1016/j.cois.2016.10.002>

581 18. Geyer PK, Corces VG. Separate regulatory elements are responsible for the complex pattern of
582 tissue-specific and developmental transcription of the yellow locus in *Drosophila melanogaster*.
583 *Genes Dev*. 1987;1: 996–1004. doi:10.1101/gad.1.9.996

584 19. Martin M, Meng YB, Chia W. Regulatory elements involved in the tissue-specific expression of
585 the yellow gene of *Drosophila*. *Mol Gen Genet MGG*. 1989;218: 118–126.
586 doi:10.1007/BF00330574

587 20. Wittkopp PJ, Vaccaro K, Carroll SB. Evolution of yellow gene regulation and pigmentation in
588 *Drosophila*. *Curr Biol*. 2002;12: 1547–1556. doi:10.1016/S0960-9822(02)01113-2

589 21. Jeong S, Rokas A, Carroll SB. Regulation of body pigmentation by the Abdominal-B Hox protein
590 and its gain and loss in *Drosophila* evolution. *Cell*. 2006;125: 1387–1399.
591 doi:<https://doi.org/10.1016/j.cell.2006.04.043>

592 22. Roeske MJ, Camino EM, Grover S, Rebeiz M, Williams TM. *Cis*-regulatory evolution integrated
593 the Bric-à-brac transcription factors into a novel fruit fly gene regulatory network. *eLife*. 2018;7:
594 e32273. doi:[10.7554/eLife.32273](https://doi.org/10.7554/eLife.32273)

595 23. Kalay G, Lachowiec J, Rosas U, Dome MR, Wittkopp P. Redundant and cryptic enhancer
596 activities of the *Drosophila yellow* gene. *Genetics*. 2019;212: 343–360.
597 doi:[10.1534/genetics.119.301985](https://doi.org/10.1534/genetics.119.301985)

598 24. Pool JE, Aquadro CF. The genetic basis of adaptive pigmentation variation in *Drosophila*
599 *melanogaster*. *Mol Ecol*. 2007. doi:[10.1111/j.1365-294X.2007.03324.x](https://doi.org/10.1111/j.1365-294X.2007.03324.x)

600 25. Takahashi A, Takahashi K, Ueda R, Takano-Shimizu T. Natural variation of *ebony* gene
601 controlling thoracic pigmentation in *Drosophila melanogaster*. *Genetics*. 2007;177: 1233–1237.
602 doi:[10.1534/genetics.107.075283](https://doi.org/10.1534/genetics.107.075283)

603 26. Rebeiz M, Pool JE, Kassner VA, Aquadro CF, Carroll SB. Stepwise modification of a modular
604 enhancer underlies adaptation in a *Drosophila* population. *Science* (80-). 2009.
605 doi:[10.1126/science.1178357](https://doi.org/10.1126/science.1178357)

606 27. Telonis-Scott M, Hoffmann A, Sgrò CM. The molecular genetics of clinal variation: a case study
607 of *ebony* and thoracic trident pigmentation in *Drosophila melanogaster* from eastern Australia.
608 *Mol Ecol*. 2011;20: 2100–2110. doi:<https://doi.org/10.1111/j.1365-294X.2011.05089.x>

609 28. Miyagi R, Akiyama N, Osada N, Takahashi A. Complex patterns of *cis*-regulatory
610 polymorphisms in *ebony* underlie standing pigmentation variation in *Drosophila melanogaster*.
611 *Mol Ecol*. 2015;24: 5829–5841. doi:[10.1111/mec.13432](https://doi.org/10.1111/mec.13432)

612 29. Takahashi A, Takano-Shimizu T. Divergent enhancer haplotype of *ebony* on inversion
613 *In(3R)Payne* associated with pigmentation variation in a tropical population of *Drosophila*
614 *melanogaster*. *Mol Ecol*. 2011;20: 4277–4287. doi:[10.1111/j.1365-294X.2011.05260.x](https://doi.org/10.1111/j.1365-294X.2011.05260.x)

615 30. Bastide H, Betancourt A, Nolte V, Tobler R, Stöbe P, Futschik A, et al. A genome-wide,

616 fine-scale map of natural pigmentation variation in *Drosophila melanogaster*. PLoS Genet. 2013.

617 doi:10.1371/journal.pgen.1003534

618 31. Dembeck LM, Huang W, Magwire MM, Lawrence F, Lyman RF, Mackay TFC. Genetic
619 architecture of abdominal pigmentation in *Drosophila melanogaster*. PLoS Genet. 2015;11: 1–22.
620 doi:10.1371/journal.pgen.1005163

621 32. Telonis-Scott M, Hoffmann AA. Enhancing *ebony*? Common associations with a *cis*-regulatory
622 haplotype for *Drosophila melanogaster* thoracic pigmentation in a Japanese population and
623 Australian populations. Front Physiol. 2018;9: 1–10. doi:10.3389/fphys.2018.00822

624 33. Mackay TFC, Richards S, Stone EA, Barbadilla A, Ayroles JF, Zhu D, et al. The *Drosophila*
625 *melanogaster* Genetic Reference Panel. Nature. 2012. doi:10.1038/nature10811

626 34. Hughes JT, Williams ME, Johnson R, Grover S, Rebeiz M, Williams TM. Gene regulatory
627 network homoplasy underlies recurrent sexually dimorphic fruit fly pigmentation. Front Ecol
628 Evol. 2020;8: 80. doi: 10.3389/fevo.2020.00080

629 35. Markow TA, O’Grady PM. *Drosophila*: a guide to species identification and use. Amsterdam:
630 Elsevier; 2006.

631 36. Halfon MS. Studying transcriptional enhancers: the founder fallacy, validation creep, and other
632 biases. Trends Genet. 2019;35: 93–103. doi:10.1016/j.tig.2018.11.004

633 37. Hsouna A, Lawal HO, Izevbaye I, Hsu T, O’Donnell JM. *Drosophila* dopamine synthesis
634 pathway genes regulate tracheal morphogenesis. Dev Biol. 2007;308: 30–43.
635 doi:<https://doi.org/10.1016/j.ydbio.2007.04.047>

636 38. Suh J, Jackson FR. *Drosophila* Ebony activity is required in glia for the circadian regulation of
637 locomotor activity. Neuron. 2007. doi:10.1016/j.neuron.2007.06.038

638 39. Pérez MM, Schachter J, Berni J, Quesada-Allué LA. The enzyme NBAD-synthase plays diverse
639 roles during the life cycle of *Drosophila melanogaster*. J Insect Physiol. 2010;56: 8–13.
640 doi:<https://doi.org/10.1016/j.jinsphys.2009.08.018>

641 40. Osterwalder M, Barozzi I, Tissières V, Fukuda-Yuzawa Y, Mannion BJ, Afzal SY, et al.

642 Enhancer redundancy provides phenotypic robustness in mammalian development. *Nature*.
643 2018;554: 239–243. doi:10.1038/nature25461

644 41. Gray S, Levine M. Transcriptional repression in development. *Curr Opin Cell Biol*. 1996;8: 358–
645 364. doi:10.1016/S0955-0674(96)80010-X

646 42. Courey AJ, Jia S. Transcriptional repression: the long and the short of it. *Genes Dev*. 2001;15:
647 2786–2796. doi:10.1101/gad.939601

648 43. Maston GA, Evans SK, Green MR. Transcriptional regulatory elements in the human genome.
649 *Annu Rev Genomics Hum Genet*. 2006;7: 29–59. doi:10.1146/annurev.genom.7.080505.115623

650 44. Ogiyama Y, Schuettengruber B, Papadopoulos GL, Chang J-M, Cavalli G. Polycomb-dependent
651 chromatin looping contributes to gene silencing during *Drosophila* development. *Mol Cell*.
652 2018;71: 73-88.e5. doi:10.1016/j.molcel.2018.05.032

653 45. Gisselbrecht SS, Palagi A, Kurland J V., Rogers JM, Ozadam H, Zhan Y, et al. Transcriptional
654 silencers in *Drosophila* serve a dual role as transcriptional enhancers in alternate cellular contexts.
655 *Mol Cell*. 2020;77: 324-337.e8. doi:10.1016/j.molcel.2019.10.004

656 46. Kopp A, Blackman RK, Duncan I. Wingless, decapentaplegic and EGF receptor signaling
657 pathways interact to specify dorso-ventral pattern in the adult abdomen of *Drosophila*.
658 *Development*. 1999;126: 3495–3507. Available: <http://dev.biologists.org/content/126/16/3495>.

659 47. Kopp A, Duncan I. Control of cell fate and polarity in the adult abdominal segments of
660 *Drosophila* by optomotor-blind. *Development*. 1997;124: 3715–3726. Available:
661 <http://dev.biologists.org/content/124/19/3715>.

662 48. Wittkopp PJ, Carroll SB, Kopp A. Evolution in black and white: genetic control of pigment
663 patterns in *Drosophila*. *Trends Genet*. 2003;19: 495–504. doi:10.1016/S0168-9525(03)00194-X

664 49. Hamaratoglu F, Affolter M, Pyrowolakis G. Dpp/BMP signaling in flies: from molecules to
665 biology. *Semin Cell Dev Biol*. 2014;32: 128–136.
666 doi:<https://doi.org/10.1016/j.semcd.2014.04.036>

667 50. Rogers WA, Grover S, Stringer SJ, Parks J, Rebeiz M, Williams TM. A survey of the

668 trans-regulatory landscape for *Drosophila melanogaster* abdominal pigmentation. *Dev Biol.*
669 2014;385: 417–432. doi:10.1016/j.ydbio.2013.11.013

670 51. Wittkopp PJ, Williams BL, Selegue JE, Carroll SB. *Drosophila* pigmentation evolution: divergent
671 genotypes underlying convergent phenotypes. *Proc Natl Acad Sci U S A.* 2003;100: 1808–1813.
672 doi:10.1073/pnas.0336368100

673 52. Lamb AM, Wang Z, Simmer P, Chung H, Patricia J, States U, et al. *ebony* affects pigmentation
674 divergence and cuticular hydrocarbons in *Drosophila americana* and *D. novamexicana*. *Front*
675 *Ecol Evol.* 2020;8: 184.

676 53. Johnson WC, Ordway AJ, Watada M, Pruitt JN, Williams TM, Rebeiz M. Genetic changes to a
677 transcriptional silencer element confers phenotypic diversity within and between *Drosophila*
678 species. *PLOS Genet.* 2015;11: e1005279. Available:
679 <https://doi.org/10.1371/journal.pgen.1005279>

680 54. Hinaux H, Bachem K, Battistara M, Rossi M, Xin Y, Jaenichen R, et al. Revisiting the
681 developmental and cellular role of the pigmentation gene *yellow* in *Drosophila* using a tagged
682 allele. *Dev Biol.* 2018;438: 111–123. doi:10.1016/j.ydbio.2018.04.003

683 55. Waldo GS, Standish BM, Berendzen J, Terwilliger TC. Rapid protein-folding assay using green
684 fluorescent protein. *Nat Biotechnol.* 1999;17: 691–695. doi:10.1038/10904

685 56. Port F, Bullock SL. Augmenting CRISPR applications in *Drosophila* with tRNA-flanked sgRNAs.
686 *Nature Methods.* 2016. pp. 852–854. doi:10.1038/nmeth.3972

687 57. Schneider CA, Rasband WS, Eliceiri KW. NIH Image to ImageJ: 25 years of image analysis. *Nat*
688 *Methods.* 2012;9: 671–675. doi:10.1038/nmeth.2089

689 58. R Core Team. R: a language and environment for statistical computing. Vienna, Austria. 2020.
690 URL: <http://www.r-project.org/>

691

692

693 **Figure Legend**

694 **Fig 1 Construction of the primary enhancer element (priEE) knockout strains**

695 (A) The genomic region surrounding *ebony* in Cas-0002-iso, an isogenic line carrying *nos*-Cas9. (B)
696 The genomic region surrounding *ebony* in Cas-0002-iso_*e::mCherry* is shown with the repair
697 construct for *mCherry* knock-in. (C) The genomic region surrounding *ebony* in strains with deleted
698 priEE after the removal of y^2 (Fig S2). The light blue box indicates the untranslated region (UTR) and
699 the blue box indicates the coding sequence (CDS). The red arrowhead indicates the target site of
700 guide RNA (gRNA) sequences. (D) Partial sequence alignment around the priEE fragment in the
701 control and priEE-deleted strains. $w^{III8}; e^{A1077priEE}::mCherry$ had a single T of unknown origin within
702 the deleted region.

703

704 **Fig 2 Effect of primary enhancer element (priEE) knockout on the intensity and patterns of**
705 **pigmentation**

706 (A) Images of the 5–7-day-old adult females. The red arrow indicates the area where the dark
707 pigmentation in the dorsal midline is missing. (B) Percent (%) darkness values of the thorax
708 measured at the area enclosed in the yellow square. (C) Percent (%) darkness values of the A4
709 abdominal segment measured at the area enclosed in the yellow square. $N = 10$ for each strain.
710 Different letters indicate significant differences between strains ($P < 0.05$; one-way analysis of
711 variance, followed by Tukey HSD post-hoc test). Error bars denote standard error.

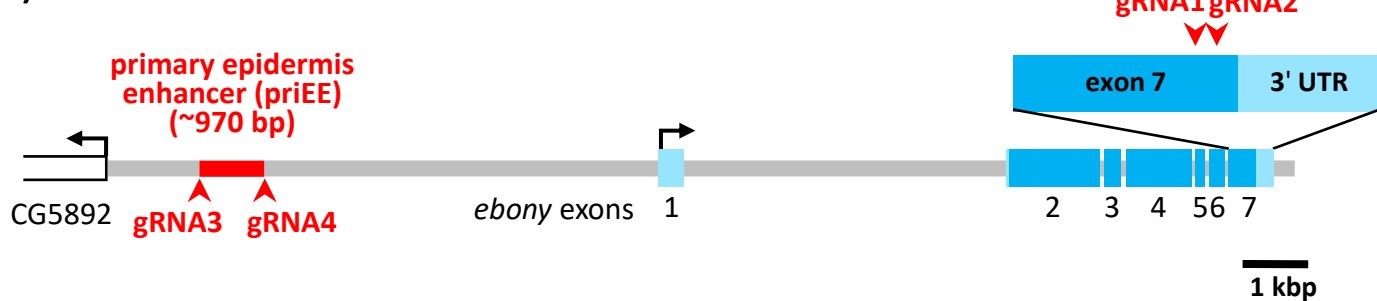
712

713 **Fig 3 cis-regulatory elements (CREs) regulate *ebony* expression in the developing epidermis**

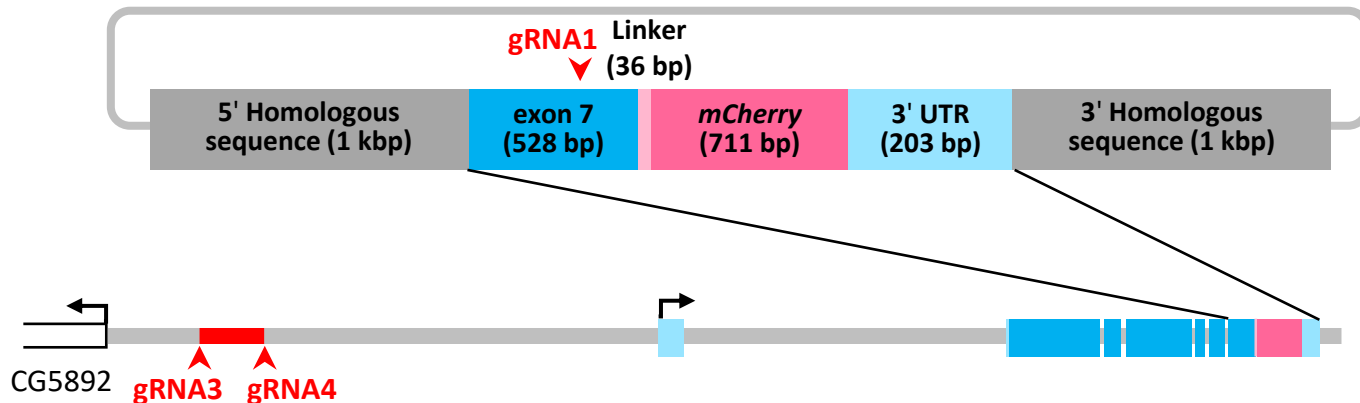
714 Confocal fluorescence images of the developing abdominal epidermis of $w^{III8}; e::mCherry$ (A),
715 $w^{III8}; e^{A1077priEE}::mCherry$ (B), and *priEE-EGFP* transformed to VK00033 (C). (D) Bright-field
716 images of (C). Images of females and males are shown in the upper and lower panels, respectively.
717 The red arrowhead indicates the dorsal midline. The yellow arrowhead indicates a dark stripe on the
718 posterior area of each tergite. The yellow bracket indicates male-specific dark pigmentation in the
719 A5 and A6 tergites. (E) Summary of the *ebony* expression sites for each strain determined from the

720 fluorescence signals. (F) The suggested model for the regulation of *ebony* expression in the abdomen.
721 The solid lines indicate the effects of priEE, while the dotted lines indicate the effects of other
722 redundant CREs. The priEE fragment was also equipped to function as a midline silencer.

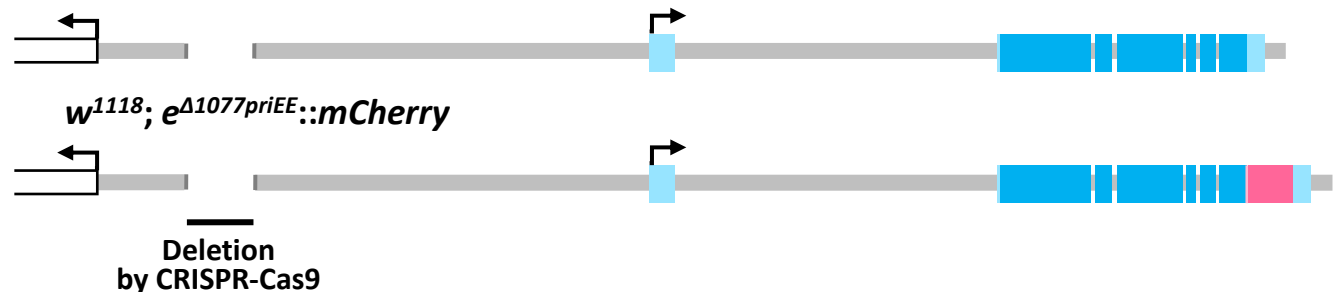
(A) Cas-0002-iso



(B) Repair construct and Cas-0002-iso_e::mCherry



(C) $w^{1118}; e^{\Delta 1088priEE}$ and $w^{1118}; e^{\Delta 1089priEE}$



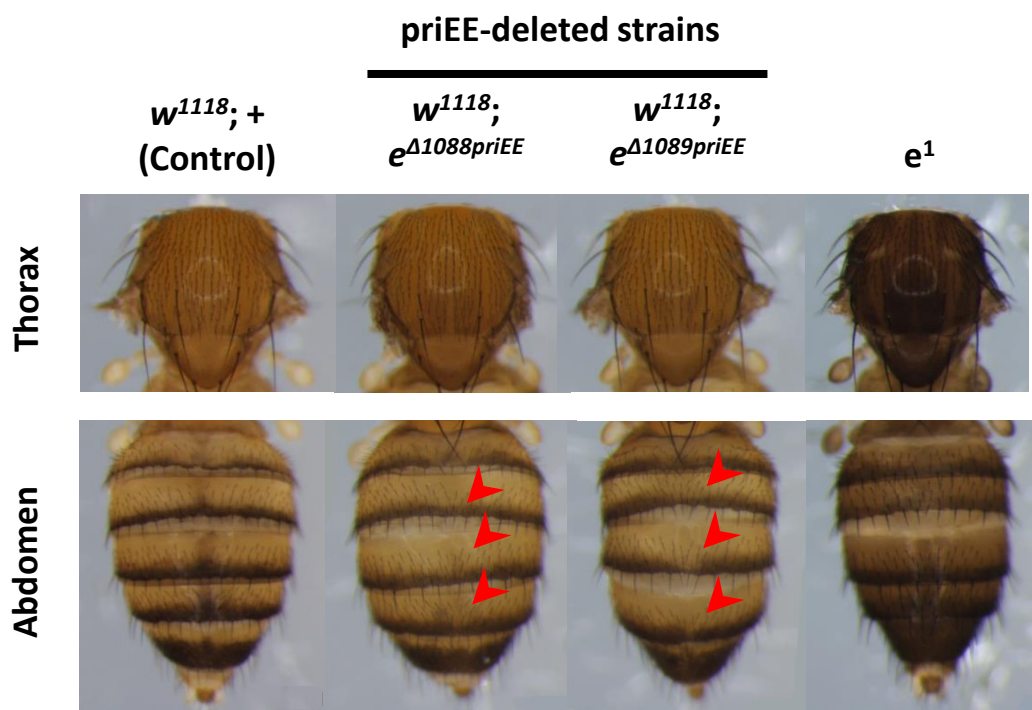
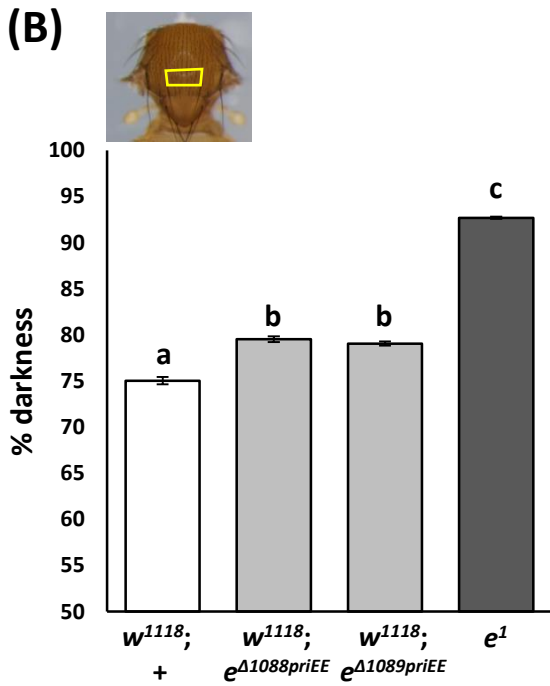
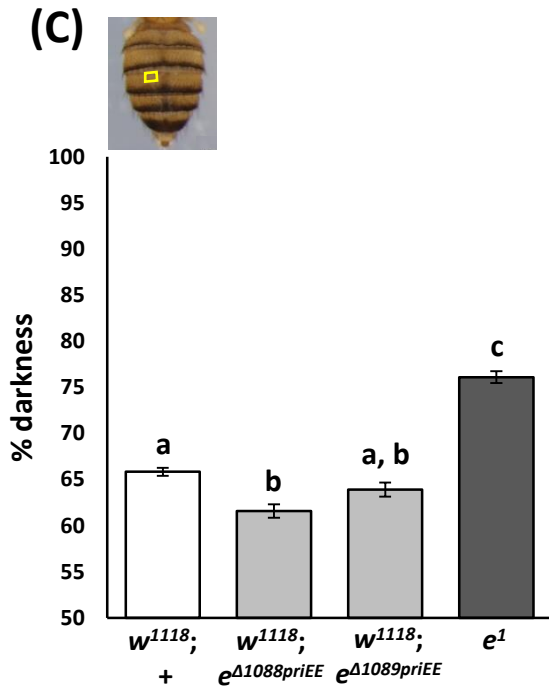
(D)

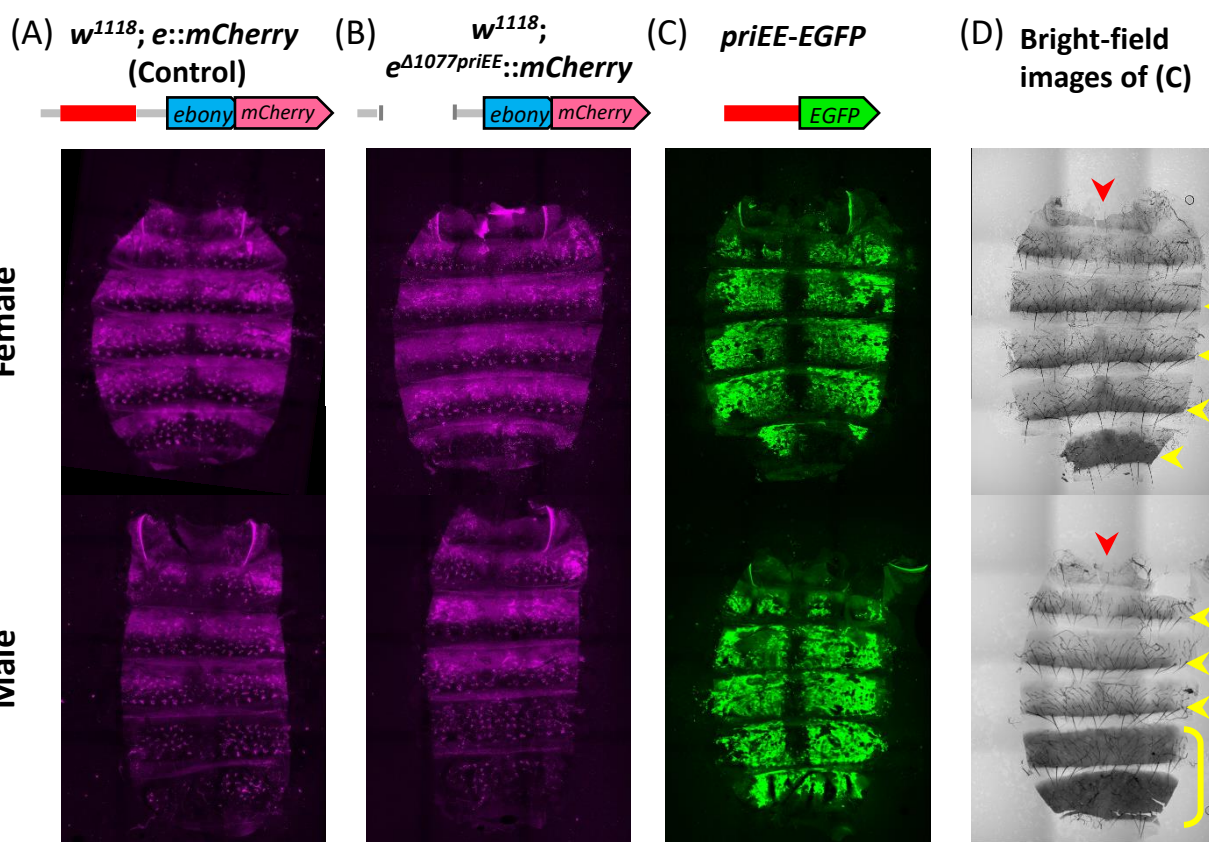
priEE (~970 bp)

gRNA3 target sequence

gRNA4 target sequence

	priEE (~970 bp)	
	gRNA3 target sequence	gRNA4 target sequence
Control ($w^{1118}; +$)	AATGTTAATAAGATCGGACAGACGGGCAA.....	ATTTTGAGAAAGTACTATCAATATAACAGG
$e^{\Delta 1088priEE}$	AATGTTAATAAG-----	AAGG-----
$e^{\Delta 1089priEE}$	AATGTTAATAAG-----	AGG-----
$e^{\Delta 1077priEE::mCherry}$	AATGTTAATAAGATCGGACT-----	TACAAGG-----
		(1,044 bp)

(A)**(B)****(C)**



Broad abdominal expression	+	+	+
Dorsal midline expression	-	+	-
Stripe expression	-	-	+
Posterior segment expression in male	-	-	+

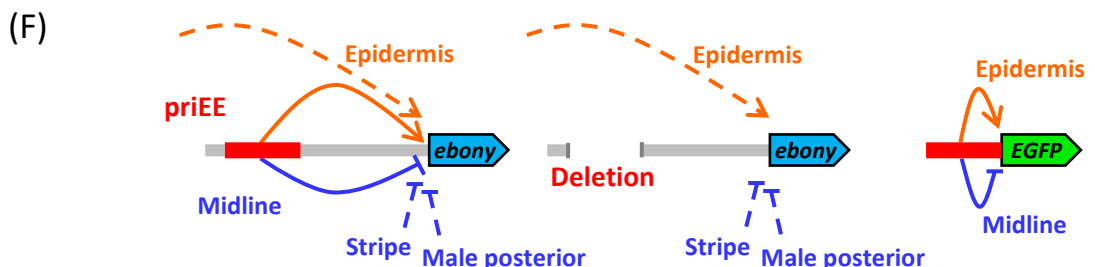


Table S1 Raw pigmentation scores (10 females per strain) of the strains used in this study

strain	Individual number	Thorax			Abdomen		
		mode	BG	%darkness ^a	mode	BG	%darkness
<i>w</i> ¹¹¹⁸ ; + (control)	1	85	161	73.5	108	162	66.5
	2	89	162	72.4	109	162	66.2
	3	79	163	75.7	114	163	64.9
	4	83	164	74.6	110	162	65.9
	5	80	162	75.2	108	162	66.5
	6	78	161	75.7	108	163	66.7
	7	76	162	76.5	116	162	64.1
	8	81	162	74.9	120	163	63.0
	9	79	162	75.5	105	161	67.3
	10	76	161	76.3	106	162	67.2
<i>w</i> ¹¹¹⁸ ; <i>e</i> ^{Δ1088priEE}	1	66	160	79.3	119	160	62.7
	2	63	161	80.4	120	159	62.1
	3	67	159	78.8	131	160	58.9
	4	66	160	79.3	133	160	58.3
	5	60	161	81.3	121	161	62.3
	6	67	160	79.0	124	163	61.8
	7	71	161	77.9	133	162	58.8
	8	64	161	80.0	111	163	65.8
	9	67	160	79.0	122	162	62.2
	10	63	161	80.4	119	161	62.9
<i>w</i> ¹¹¹⁸ ; <i>e</i> ^{Δ1089priEE}	1	66	159	79.2	117	160	63.3
	2	68	160	78.7	112	159	64.6
	3	66	160	79.3	108	163	66.7
	4	64	161	80.0	107	160	66.4
	5	69	160	78.4	117	160	63.3
	6	68	160	78.7	109	160	65.8
	7	64	160	79.9	119	161	62.9
	8	71	161	77.9	116	161	63.8
	9	65	161	79.7	133	160	58.3
	10	68	161	78.8	117	163	64.0
<i>e</i> ¹	1	25	159	92.1	88	159	72.2
	2	24	161	92.5	86	159	72.8
	3	23	160	92.8	76	158	75.9
	4	22	161	93.1	70	159	77.9
	5	23	160	92.8	69	159	78.2
	6	23	161	92.8	70	159	77.9
	7	25	158	92.1	73	159	77.0
	8	23	159	92.7	74	160	76.8
	9	21	160	93.4	76	161	76.3
	10	24	160	92.5	76	159	76.0

mode: grayscale mode of quantified area; BG: gray background area

^a % darkness was calculated from mode and BG.

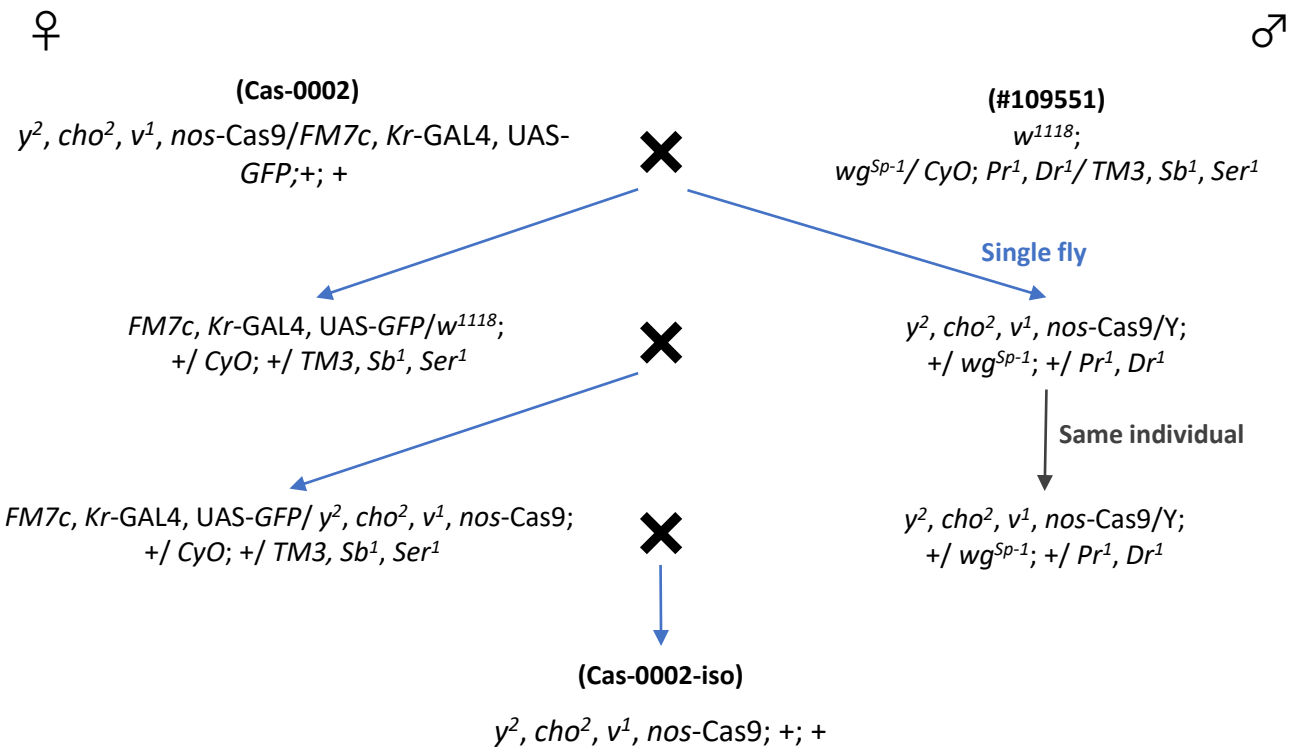


Fig S1 Scheme for extracting an isogenized chromosome

To control for the genetic background of the genome-edited flies, each chromosome was originated from a single chromosome. The isogenized strain was named Cas-0002-iso.

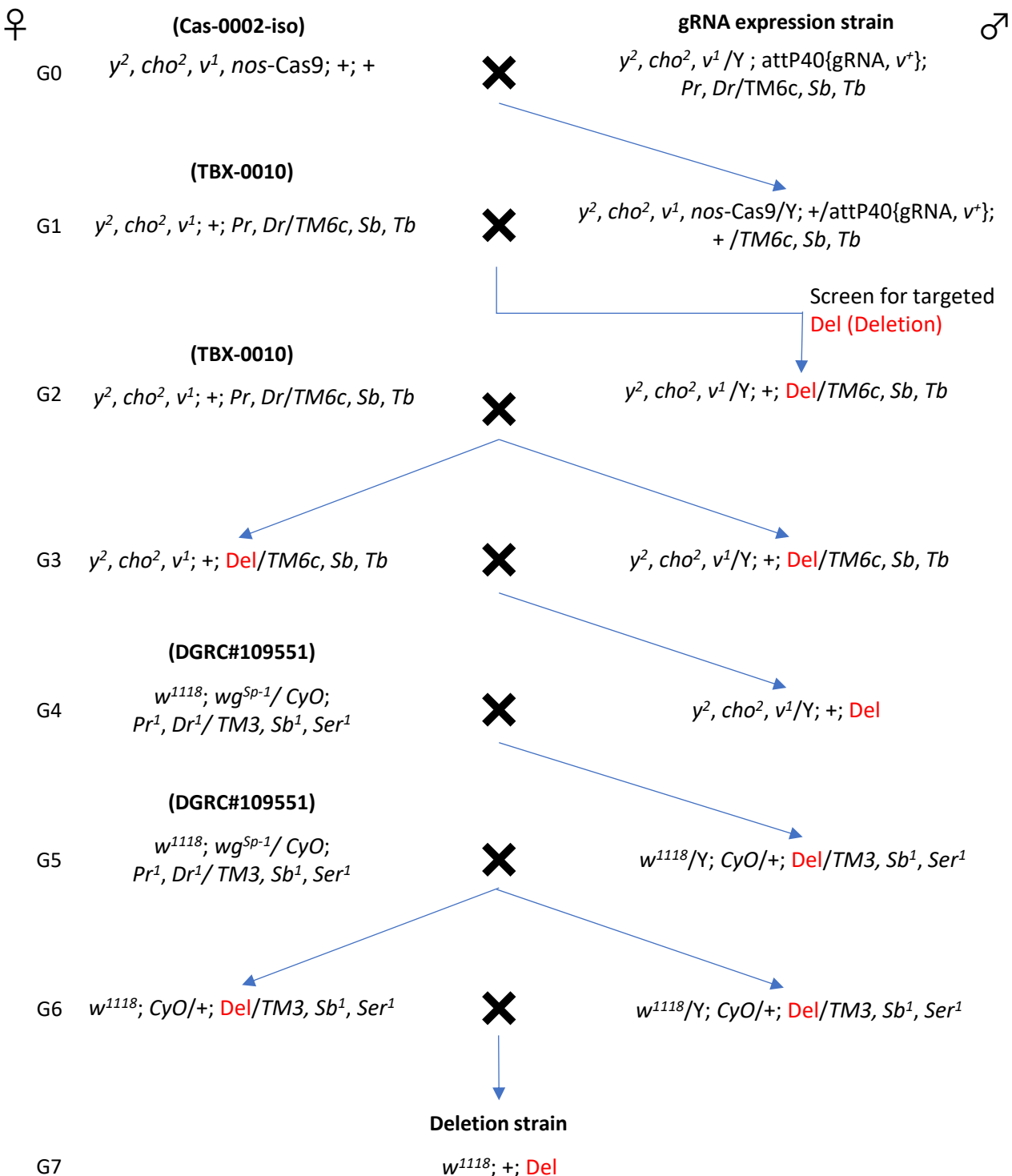


Fig S2 Scheme for generating primary enhancer element (priEE) deletion strains without y^2

CRISPR-Cas9-based genome editing was performed by crossing the Cas-0002-iso with the guide RNA (gRNA) expression strain (G0). The progenies from the G1 cross were screened for the presence of deletions. Homologous deletions were achieved by the crosses in G3 and G4. y^2 was removed by the crosses in G4 to G7 because it interferes with *ebony* in the pigment biosynthesis pathway. Deletion strains for mCherry fluorescence observation were established using the same scheme, except Cas-0002-iso_e::mCherry was used instead of Cas-0002-iso (G0). Control strains ($w^{1118}; +; +$ and $w^{1118}; +; e::mCherry$) were established with the same crosses using TBX-0002 instead of the gRNA expression strain and using + instead of the Del genotype for the G2 cross.

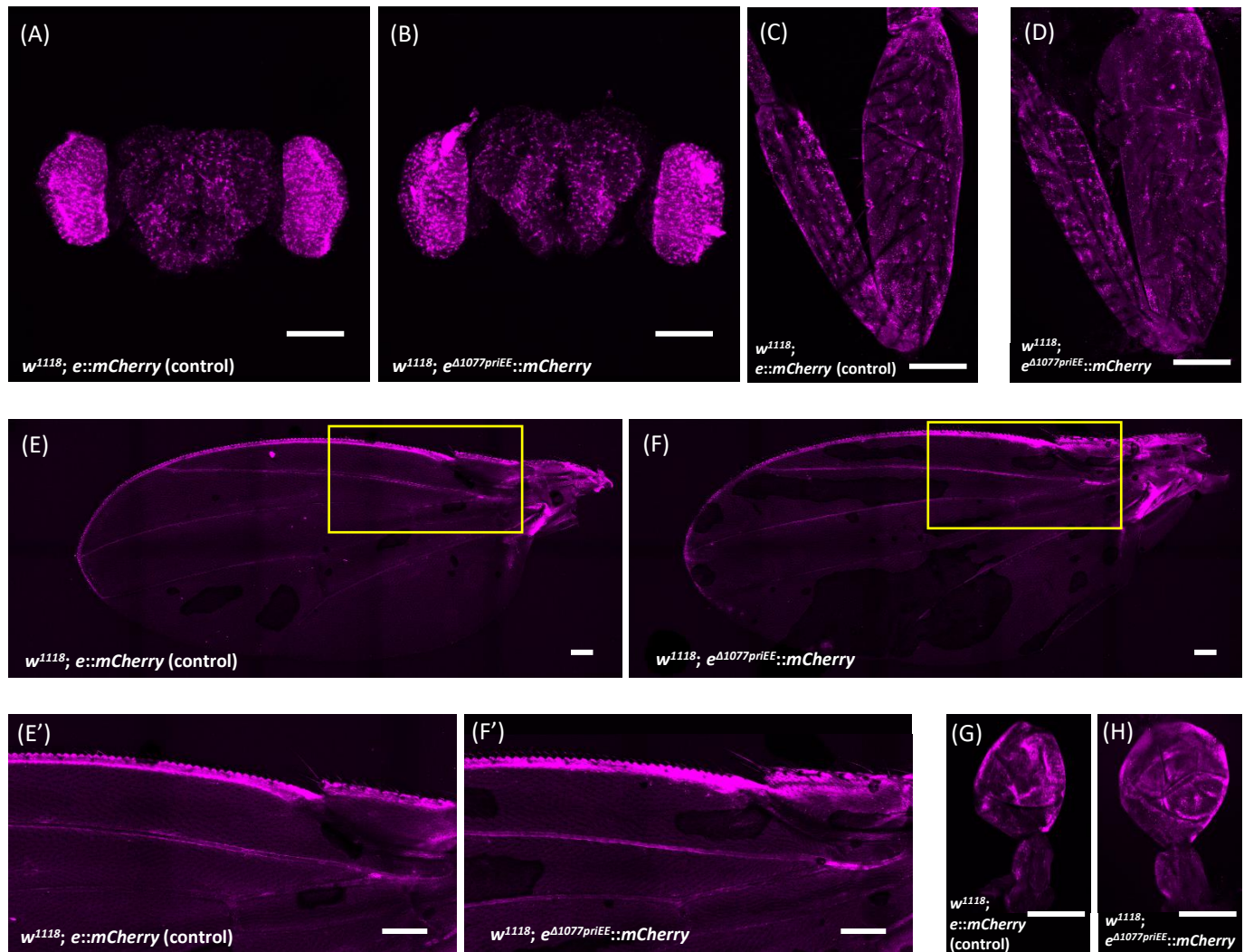


Fig S3 ebony expression in tissues other than developing epidermis

Confocal images of brain (A and B), front leg (C and D), wing (E, E', F and F'), and haltere (G and H). Each tissue was dissected from the control, $w^{1118}; e::mCherry$ (A, C, E, E' and G), and the priEE-deleted strain $w^{1118}; e^{\Delta 1077priEE}::mCherry$ (B, D, F, F' and H). (E') and (F') are magnified views of the yellow square in (E) and (F), respectively. The scale bars indicate 100 μ m.

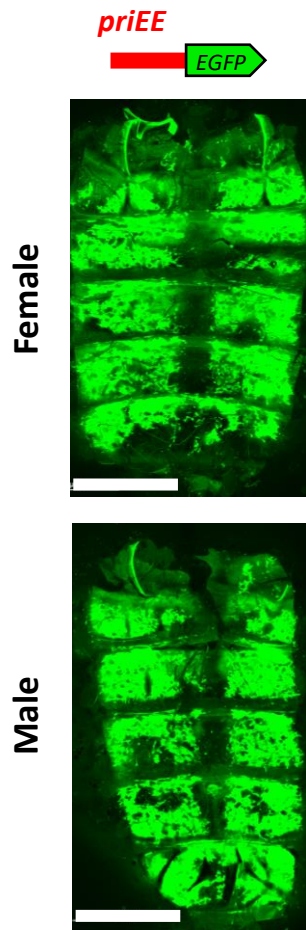


Fig S4 Reporter assay using the enhanced GFP-tagged primary enhancer element (*priEE-EGFP*) construct in the developing abdominal epidermis

Confocal fluorescence images of the developing abdominal epidermis of *priEE-EGFP* transformed to VK00037. Images of females and males are shown in the upper and lower panels, respectively.. Scale bars indicate 500 μ m.

gRNA3 target sequence

1 TTTTAATTATTCGGATTTAATGTTAATAAGATCGGACAGACGGGCAAAGCAGGGTGAATTTGATAACGTTCAAGTATTATGGCCCGGA
e^{A1029}priEE TTTTAATTATTCGGATTTAATGTTAATAAG-----
e^{A1030}priEE TTTTAATTATTCGGATTTAATGTTAATAAG-----
e^{A1018}priEE TTTTAATTATTCGGATTTAATGTTAATAAGATCGGACT-----

101 **AACGCATCCATTACCTGCTGCATACTTTCAACGAGTCTAATATGTCATACTTTACCCCTCAAGTAACGGCTATGGAAGTATTGTAACACCTT**

201 **CTTATCTATCAAAGTCTGGTAATTCAAAAACGCCTGTGCCCATCGAATCGTTCTCAGGTGCTTTTATTACTTTGATGAAGTAGATGCAATCAGTG**

301 **CGGAAAGTTGATAGCGAGTATATCTTAATAATCGATCTTCATTAGTAATTAACATAAGTCTGGTTTGAGTGAAACTGATAGACTGAATAGTG**

401 **ATCAGCTGGTGTGGCTGCAACTTGTCAACCATTAATATATGGTGTGGTAAATCATGAATGCATCTTAATGGTAGTGAAACTTGTCAACCATTAATATATG**

501 **GTGTGGTAAATCATGAATGCATCTTAATGGTAGTGAAATTAAATCGCTTAATTCAATTAAACACATTTTTACTCGTAAGTCGTAGATTAAAATTAT**

601 **GTAACAGATAGGATAGAGGATTTAGTCCTATAAAGTATAAGTATTCTGGCTTATCCGTATGAGCATCCATATACAGAAATATGGATTGTTT**

701 **CAAACAACGTCCACACTTTAAAAATGTTCCATTTCATTTCATTATAATTATCATTCAATTCAATTCCAAAGTTGTCAATC**

801 **CATCAGTAAACAAGTCGGCTAGAGATGTTGATTAAGAAGAGCTTACATTATAAAACAAAATACGAAATTAAATAGTAGCTGCCCTTCCTTATAGGA**

901 **ATTAAATTATTTTATGACTTACCAATTTCATTAAACGGCATAGATATTCCAAATCAATTGAGGGTAGAGGCTGTAAAAGTCATTGAAC**

1001 **TAAGCTTGCAAGCTAATTCTATGTTCTAACGGATACTAATCTTATTCCCCATTCAATCTAAACAGAAAATTCCATAAGTCCCTGTGATTGATT**

gRNA4 target sequence

1101 **TGAGAAAGTACTATCAATATACAAGGAAGCATTCTGTGCTACATCGAATCCTAATAAAACTGAATACCTAAAGGATAA**
-----**AAGGAAGCATTCTGTGCTACATCGAATCCTAATAAAACTGAATACCTAAAGGATAA**
-----**AGGAAGCATTCTGTGCTACATCGAATCCTAATAAAACTGAATACCTAAAGGATAA**
-----**TACAAGGAAGCATTCTGTGCTACATCGAATCCTAATAAAACTGAATACCTAAAGGATAA**

Fig S5 Alignment of sequences around the primary enhancer element (priEE) in the control and priEE knockout strains

The guide RNA (gRNA) target sequences are indicated above the sequence. Bases in bold indicate the 947-bp sequence of e_ECR0.9 from Takahashi and Takano-Shimizu [29] (969-bp sequence in the control strain (Cas-0002-iso-derived *w*¹¹¹⁸; + strain)). Bases in blue indicate the 961-bp sequence of e_core_cis sequence from Miyagi *et al.* [28] (975 bp in the control strain (Cas-0002-iso-derived *w*¹¹¹⁸; + strain)). Shaded bases indicate the sequence fragment (1,047 bp) used for the reporter assay in this study.